IEEE Access
Multidisciplinary : Rapid Review : Open Access Journal

Received November 24, 2018, accepted February 2, 2019, date of publication February 11, 2019, date of current version February 27, 2019.

Digital Object Identifier 10.1109/ACCESS.2019.2898457

Analysis and Mitigation of ICI Due to Gain Adjustment in OFDM Systems

HAO WU[1,2], (Member, IEEE), AND JUN LI[1]
[1]Wireless Product Research and Design Institute, ZTE Corporation, Shenzhen 518055, China
[2]State Key Laboratory of Mobile Network and Mobile Multimedia Technology, ZTE Corporation, Shenzhen 518055, China

Corresponding author: Hao Wu (wu.hao19@zte.com.cn)

ABSTRACT Automatic gain control (AGC) is widely adopted in orthogonal frequency division multiplexing (OFDM) systems to compensate the significant variation of the received signal. In OFDM systems, the duration of the cyclic prefix (CP) is usually equal to the delay spread of the channel to minimize the system overhead. The inter-symbol interference (ISI) between consecutive OFDM symbols spreads over a large portion of the CP. The CP contaminated by the ISI should not be used to estimate the received power. If the duration of the remaining CP is shorter than the settling time of the AGC, then the gain adjustment will be carried out within the useful portion of the OFDM symbol. The subcarrier orthogonality is lost and the system performance is degraded by the resulting inter-carrier interference (ICI). In this paper, we propose a simple and efficient scheme to mitigate the ICI. The proposed scheme can be easily implemented in actual systems because of its low computational complexity. The simulation results show that the proposed scheme can increase the signal-to-interference-plus-noise ratio significantly compared to the traditional scheme.

INDEX TERMS Automatic gain control, inter-carrier interference, inter-symbol interference, orthogonal frequency division multiplexing.

I. INTRODUCTION

Orthogonal frequency division multiplexing (OFDM) is a popular scheme for communication systems. In OFDM systems, the received signal can vary over a large dynamic range due to variations of the transmit power and the path loss. Automatic gain control (AGC) is widely used in OFDM systems to make the power of the received signal approximately constant, so that the quantization error caused by the analog to digital converter (ADC) is minimized. And OFDM systems have a stringent requirement for the AGC in terms of the settling time.

AGC usually consists of three modules: a variable gain amplifier (VGA), a power detector and a loop filter [1]. The VGA adjusts the power of the received signal depending on the control signal. The other two modules belong to the control loop. The power detector estimates the received power. The loop filter provides the control signal, which is determined by the difference between the estimated power and the target power. AGC can be roughly divided into two categories according to whether the control loop is analog or digital. For the first category [2]–[4], the power detector and the loop filter are typically based on the analog circuit. For the second category [5]–[7], the power detector and the loop filter are typically based on the digital circuit. The analog AGC is specific and complex. The digital AGC is generic and simple. Each category has its own advantages and disadvantages. The gain of the VGA can be converged in one step [8], [9]. The one step scheme shortens the settling time of the AGC. At the same time, the one step scheme simplifies the analysis of the impact of the gain adjustment on OFDM systems. In this paper, the gain of the VGA is assumed to be adjusted in one step.

In OFDM systems, the duration of the cyclic prefix (CP) is usually equal to the delay spread of the channel to minimize the system overhead [10]. Due to the multipath effect, the inter-symbol interference (ISI) between consecutive OFDM symbols spreads over a large portion of the CP. In some scenarios, there is a large difference between received powers of consecutive OFDM symbols [11], [12]. As a result, the CP contaminated by the ISI should not be used to estimate the received power. If the duration of the remaining CP is shorter than the settling time of the AGC, then the gain adjustment will be carried out within the useful

The associate editor coordinating the review of this manuscript and approving it for publication was Vivek Ashok Bohara.

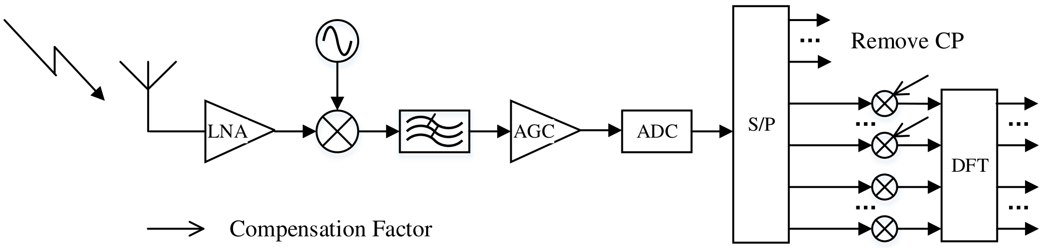

FIGURE 1. The architecture of the proposed scheme to mitigate the ICI due to the gain adjustment in OFDM systems. The proposed scheme adjusts the power of the received signal after the ADC.

portion of the OFDM symbol. The subcarrier orthogonality is lost and the system performance is degraded by the resulting inter-carrier interference (ICI) [11], [13]. This problem is more serious for OFDM systems without CP [14], [15] or with insufficient CP [16], [17]. The ICI should be mitigated to improve the system performance.

The traditional scheme of the AGC does not consider the mitigation of the ICI due to the gain adjustment in OFDM systems [8], [18]. The ICI degrades the performance of the traditional scheme. References [13] and [19] force the power of the received signal to be adjusted within the CP. The settling time presents a significant challenge for the AGC design when the duration of the CP is short. The abrupt change of the gain is a specific time-varying channel. It is well known that the ICI is generated in the time-varying channel. A lot of schemes have been proposed to mitigate this kind of the ICI [20]–[23]. However, the schemes proposed in [20]–[23] cannot be directly applied to mitigate the ICI due to the gain adjustment in OFDM systems. The scenario considered in [20]–[23] is that equivalent channel filter taps during an OFDM symbol interval change continuously and independently. The scenario considered in this paper is that equivalent channel filter taps during an OFDM symbol interval change only once simultaneously. In addition, [20]–[23] do not take the nonlinear effect of the ADC into consideration.

In this paper, we propose a simple and efficient scheme to mitigate the ICI due to the gain adjustment in OFDM systems. Fig. 1 illustrates the architecture of the proposed scheme. To correct the behavior of the AGC, part of the output of the ADC is multiplied by a compensation factor before being fed into the discrete Fourier transformation (DFT) block. The compensation factor reduces the discontinuity of the received signal after the gain adjustment within the useful portion of the OFDM symbol. The computational complexity of the proposed scheme is linear in the number of subcarriers in the useful portion of the OFDM symbol. Due to the low computational complexity, the proposed scheme can be easily implemented in actual systems.

The rest of the paper is organized as follows. We derive the signal-to-interference-plus-noise ratio (SINR) when the gain is adjusted within the useful portion of the OFDM symbol in Section II. The proposed scheme to mitigate the ICI due to the gain adjustment is given in Section III. Section IV considers implementation issues of the proposed scheme. The simulation results are presented in Section V. And Section VI concludes the paper.

II. SYSTEM MODEL

Let $\widetilde{\mathbf{x}} = [\widetilde{x}_0, \widetilde{x}_1, \ldots, \widetilde{x}_{N-1}]^{\mathrm{t}}$ be the transmit signal in the frequency domain, where N is the total subcarriers of the OFDM system and $(\cdot)^{\mathrm{t}}$ denotes the transpose of the enclosed vector. We assume that $\widetilde{\mathbf{x}}$ is a sequence of independent and identically distributed random variables with mean 0 and variance N_x [24], [25]. By the inverse discrete Fourier transformation (IDFT), $\widetilde{\mathbf{x}}$ is transformed into the time domain $\mathbf{x} = [x_0, x_1, \ldots, x_{N-1}]^{\mathrm{t}}$, where

$$x_j = \frac{1}{\sqrt{N}} \sum_{k=0}^{N-1} \widetilde{x}_k e^{\frac{\mathrm{i}2\pi kj}{N}} \quad j = 0, 1, \ldots, N-1 \tag{1}$$

and i is equal to $\sqrt{-1}$. $\mathbf{x}$ is approximately distributed as $\mathcal{CN}(\mathbf{0}_{N\times 1}, N_x\mathbf{I}_N)$ when N is much larger than 1 [26], where $\mathbf{0}_{N\times 1}$ denotes the $N \times 1$ zero matrix, $\mathbf{I}_N$ denotes the $N \times N$ identity matrix and $\mathcal{CN}(\mathbf{0}_{N\times 1}, N_x\mathbf{I}_N)$ denotes the circularly symmetric complex Gaussian random vector with mean $\mathbf{0}_{N\times 1}$ and covariance matrix $N_x\mathbf{I}_N$. After the attachment of the CP of length $(L-1)$, the time domain signal is transmitted over the air.

Let $\mathbf{w} = [w_0, w_1, \ldots, w_{N-1}]^{\mathrm{t}}$ be the additive white Gaussian noise (AWGN) on the useful portion of the OFDM symbol. $\mathbf{w}$ is modeled as $\mathcal{CN}(\mathbf{0}_{N\times 1}, N_0\mathbf{I}_N)$, where N_0 is the power spectral density of the white Gaussian noise. Let $\mathbf{h} = [h_0, h_1, \ldots, h_{\mathcal{L}-1}]^{\mathrm{t}}$ be the channel filter taps, where $\mathcal{L}$ is the delay spread of the channel. $\mathbf{h}$ is modeled as $\mathcal{CN}(\mathbf{0}_{\mathcal{L}\times 1}, \mathrm{diag}(\sigma_0, \sigma_1, \ldots, \sigma_{\mathcal{L}-1}))$, where σ_j is the power of the jth channel filter tap and $\mathrm{diag}(\cdot)$ denotes the diagonal matrix with the entries of the enclosed vector on its main diagonal. Let $\mathbf{y} = [y_0, y_1, \ldots, y_{N-1}]^{\mathrm{t}}$ be the received signal of the useful portion of the OFDM symbol after the gain adjustment. If $\mathcal{L}$ is smaller than or equal to L and the power of the received signal is adjusted just before receiving y_n, then we have

$$y_j = \begin{cases} \sum_{l=0}^{\mathcal{L}-1} h_l x_{\mathrm{mod}(j-l,N)} + w_j & j = 0, \ldots, n-1 \\ \sum_{l=0}^{\mathcal{L}-1} g h_l x_{\mathrm{mod}(j-l,N)} + g w_j & j = n, \ldots, N-1 \end{cases} \tag{2}$$

$$\begin{aligned}\widetilde{y}_j &= \frac{1}{N}\sum_{p=0}^{N-1}\widetilde{h}_p\widetilde{x}_p(\sum_{k=0}^{n-1}s_f e^{-\frac{i2\pi(j-p)k}{N}}) + \frac{1}{N}\sum_{p=0}^{N-1}\widetilde{h}_p\widetilde{x}_p(\sum_{k=n}^{N-1}gs_o e^{-\frac{i2\pi(j-p)k}{N}}) + \widetilde{w}_j \\ &\overset{(I)}{=} \frac{s_f n + gs_o(N-n)}{N}\widetilde{h}_j\widetilde{x}_j + \frac{gs_o - s_f}{N}\sum_{p=0,p\neq j}^{N-1}\widetilde{h}_p\widetilde{x}_p e^{-\frac{i\pi(j-p)(N+n-1)}{N}}S(j-p,n) + \widetilde{w}_j \end{aligned} \tag{9}$$

where g is the gain of the AGC and n is the position of the gain adjustment. It is clear that $0 < g < \infty$ and $0 < n < N-1$. Let

$$P = N_0 + N_x \sum_{l=0}^{\mathcal{L}-1}|h_l|^2 \tag{3}$$

y_j is distributed as $\mathcal{CN}(0, P)$ for $j = 0, 1, \ldots, n-1$ and $\mathcal{CN}(0, g^2P)$ otherwise [27], [28]. Without loss of generality, suppose the span of the ADC is equal to 1. The clipping ratio of y_j is [29]

$$c_j = \begin{cases}\sqrt{2/P} & j = 0, \ldots, n-1 \\ \sqrt{2/(g^2P)} & j = n, \ldots, N-1\end{cases} \tag{4}$$

If c_o is the optimal clipping ratio, then g should be set to $\sqrt{2/(P'c_o^2)}$ [11], where P' is the estimate of the received power. Let $\log_2 R$ be the resolution of the ADC. In the case of the mid-riser uniform quantization, the output range of the ADC is partitioned into R disjoint intervals: $\Omega_0 = (b_0, b_1]$, $\Omega_1 = (b_1, b_2], \ldots, \Omega_{R-1} = (b_{R-1}, b_R)$, where

$$b_k = \begin{cases}2k/R - 1 & k = 1, 2, \ldots, R-1 \\ -\infty & k = 0 \\ +\infty & k = R\end{cases} \tag{5}$$

If $y_j \in \Omega_k$, then y_j is represented by $q_{k+1} = (2k+1)/R - 1$. According to the Bussgang's theorem [30], the quantized version of y_j is modelled as $\mathbb{Q}(y_j) = s_j y_j + d_j$, where s_j is the attenuation factor and d_j is the quantization noise due to the nonlinear effect of the ADC. d_j is uncorrelated with y_j. The values of s_j and $\mathrm{Var}(d_j)$ are given in [29], where $\mathrm{Var}(\cdot)$ denotes the variance of the enclosed variable. It is clear that s_j and $\mathrm{Var}(d_j)$ do not vary over the intervals of $[0, n-1]$ and $[n, N-1]$. For simplicity, let

$$s_j = \begin{cases}s_f & j \in [0, n-1] \\ s_o & j \in [n, N-1]\end{cases} \tag{6}$$

and

$$\mathrm{Var}(d_j) = \begin{cases}D_f & j \in [0, n-1] \\ D_o & j \in [n, N-1]\end{cases} \tag{7}$$

The signal-to-quantization-noise ratio (SQNR) of $\mathbb{Q}(y_j)$ is defined as $\mathrm{SQNR}_j = s_j^2\mathrm{Var}(y_j)/\mathrm{Var}(d_j)$. Since the SQNR increases after the gain adjustment, we have

$$\frac{g^2 s_o^2}{D_o}P > \frac{s_f^2}{D_f}P \tag{8}$$

The DFT of the output of the ADC is given by (9), as shown at the top of this page, where

$$\widetilde{w}_j = \sum_{k=0}^{n-1}\frac{s_f w_k + d_k}{\sqrt{N}}e^{-\frac{i2\pi jk}{N}} + \sum_{k=n}^{N-1}\frac{gs_o w_k + d_k}{\sqrt{N}}e^{-\frac{i2\pi jk}{N}} \tag{10}$$

and $\widetilde{h}_j = \sum_{l=0}^{\mathcal{L}-1}h_l e^{-\frac{i2\pi jl}{N}}$. $\widetilde{w}_j$ is the total noise (the scaled white Gaussian noise plus the quantization noise) of the jth subcarrier and $\widetilde{h}_j$ is the channel frequency response of the jth subcarrier. The following identity is used in step (I)

$$\sum_{k=n}^{N-1}e^{\frac{-i2\pi jk}{N}} = \begin{cases}N-n & j = 0 \\ e^{\frac{-i\pi j(N+n-1)}{N}}S(j,n) & j \neq 0\end{cases} \tag{11}$$

where

$$S(j,n) = \sin(\frac{(N-n)\pi j}{N})/\sin(\frac{\pi j}{N}) \tag{12}$$

The second term in the last line of (9) corresponds to the ICI, which indicates that the subcarriers in an OFDM symbol are no longer orthogonal to each other. Applying the central limit theory, we get the approximation

$$\widetilde{w}_j \sim \mathcal{CN}(0, (N_f\frac{n}{N} + N_o\frac{N-n}{N})) \tag{13}$$

where $N_f = s_f^2 N_0 + D_f$ and $N_o = g^2 s_o^2 N_0 + D_o$. N_f and N_o are the total noise powers before and after the position of the gain adjustment respectively. The SINR of the jth subcarrier is

$$\mathrm{SINR}_j = \frac{(s_f n + gs_o(N-n))^2 N_x|\widetilde{h}_j|^2}{(gs_o - s_f)^2 I(j,n) + N(N_f n + N_o(N-n))} \tag{14}$$

where $|\cdot|$ denotes the magnitude of the enclosed variable and $I(j,n)$ is equal to

$$I(j,n) = \mathrm{Var}[\sum_{p=0,p\neq j}^{N-1}\widetilde{h}_p\widetilde{x}_p e^{-\frac{i\pi(j-p)(N+n-1)}{N}}S(j-p,n)] \tag{15}$$

$(gs_o - s_f)^2 I(j,n)$ corresponds to the power of the ICI.

A. THE VALUE OF E[$I(j,n)$]

To get a feel for the value of $I(j,n)$, we derive a closed form expression for E[$I(j,n)$], where E[$\cdot$] denotes the average of the enclosed variable over the stationary distribution of the channel. In preparation of the derivation, the following lemma is established.

Lemma 1: The following equation holds for $0 < n < N-1$.

$$\sum_{p=1}^{N-1} S(p,n)^2 = -n^2 + Nn \tag{16}$$

Proof: The recursive formula of $\sum_{p=1}^{N-1} S(p,n)^2$ is

$$\sum_{p=1}^{N-1} S(p,n+1)^2 = \sum_{p=1}^{N-1} S(p,n)^2 + \sum_{p=1}^{N-1} \frac{\sin(\frac{(2n+1)\pi p}{N})}{\sin(\frac{\pi p}{N})} \tag{17}$$

and

$$\sum_{p=1}^{N-1} \frac{\sin(\frac{(2n+1)\pi p}{N})}{\sin(\frac{\pi p}{N})} = \sum_{p=1}^{N-1} \frac{\sin(\frac{(2n-1)\pi p}{N})}{\sin(\frac{\pi p}{N})} + 2\sum_{p=1}^{N-1} \cos(\frac{2n\pi p}{N})$$

Then the explicit formula of $\sum_{p=1}^{N-1} S(p,n)^2$ can be obtained as follows. First, note that

$$\sum_{p=1}^{N-1} \cos(\frac{2n\pi p}{N}) \overset{\text{(I)}}{=} -1 \tag{18}$$

where in step (I) we use the identity [31]

$$\sum_{p=1}^{N-1} \cos(p\theta) = -\frac{1}{2} + \frac{\sin(N-\frac{1}{2})\theta}{2\sin(\frac{\theta}{2})} \tag{19}$$

From the recursive formula of $\sum_{p=1}^{N-1} S(p,n)^2$ and (18), we obtain

$$\sum_{p=1}^{N-1} \frac{\sin(\frac{(2n+1)\pi p}{N})}{\sin(\frac{\pi p}{N})} = N-1-2n \tag{20}$$

and $\sum_{p=1}^{N-1} S(p,n)^2 = -n^2 + nN$. The proof is complete. □

From (15), we have

$$\begin{aligned} I(j,n) &= \sum_{p=0,p\neq j}^{N-1} N_x |\widetilde{h}_p|^2 S(j-p,n)^2 \\ &= \sum_{p=0,p\neq j}^{N-1} N_x \sum_{l=0}^{\mathcal{L}-1}\sum_{m=0}^{\mathcal{L}-1} h_l h_m^* e^{-\frac{i2\pi p(l-m)}{N}} S(j-p,n)^2 \end{aligned} \tag{21}$$

where $(\cdot)^*$ denotes the conjugation of the enclosed variable. From the preceding lemma, we obtain

$$\begin{aligned} \mathrm{E}[I(j,n)] &= \mathrm{E}[\sum_{l=0}^{\mathcal{L}-1} N_x |h_l|^2 \sum_{p=0,p\neq j}^{N-1} S(j-p,n)^2] \\ &= N_x(-n^2+Nn)\sum_{l=0}^{\mathcal{L}-1} \sigma_l \end{aligned} \tag{22}$$

The value of $\mathrm{E}[I(j,n)]$ is constant for different subcarriers in an OFDM symbol and achieves its maximum value at $n = N/2$.

III. ICI MITIGATION

From (9), it is clear that the ICI does not exist when s_f is equal to gs_o. s_f and gs_o are equal to the scalings of the received signal before and after the position of the gain adjustment respectively. We can conclude that the cause of the ICI is mainly due to the abrupt change of the input of the DFT. To mitigate the ICI, the discontinuity of the received signal after the gain adjustment should be compensated. If $\mathbb{Q}(y_0), \mathbb{Q}(y_1), \ldots, \mathbb{Q}(y_{n-1})$ are multiplied by a compensation factor before being fed into the DFT block, then the DFT input is smoothed and the ICI is mitigated. The block diagram of the proposed scheme is shown in Fig. 1.

The quantized version of the received signal before the gain adjustment is now: $\xi\mathbb{Q}(y_j) = \xi(s_f y_j + d_j)$ for $j = 0, 1, \ldots, n-1$, where ξ is the compensation factor. The attenuation factor is changed from s_f to $s_f\xi$ and the power of the quantization noise is changed from D_f to $D_f\xi^2$. The quantized version of the received signal after the gain adjustment is unchanged. Similar to the analysis of SINR_j, the SINR of the jth subcarrier of the proposed scheme is

$$\mathrm{SINR}_j(\xi) = \frac{(s_f\xi n + gs_o(N-n))^2 N_x |\widetilde{h}_j|^2}{(gs_o - s_f\xi)^2 I(j,n) + N(N_f^* n + N_o(N-n))} \tag{23}$$

where $N_f^* = (s_f\xi)^2 N_0 + D_f\xi^2$. N_f^* is the product of ξ^2 and N_f. The partial derivation of $\mathrm{SINR}_j(\xi)$ to ξ is given by (24), as shown at the bottom of this page. $\mathrm{SINR}_j(\xi)$ achieves its maximum value when ξ is equal to

$$\xi_o = \frac{s_f}{gs_o}\frac{D_o(Nn-n^2) + g^2 s_o^2(N_0(Nn-n^2) + I(j,n))}{D_f(Nn-n^2) + s_f^2(N_0(Nn-n^2) + I(j,n))} \tag{25}$$

ξ_o is the optimal compensation factor. It is very expensive to calculate ξ_o. Also, ξ_o depends on the subcarrier index, which results an impractical implementation. We need to simplify ξ_o to make the proposed scheme practical.

The resolution of the ADC is usually around 10 bits in actual systems [32], [33]. In this case, the SQNR is much larger than 1 over a wide range of clipping ratios, as illustrated in Fig. 2. The clipping ratios before and after the position of the gain adjustment fall into this range with sufficiently high probability. Thus we can safely assume that the following two expressions hold

$$D_o \ll g^2 s_o^2 (N_0 + N_x \sum_{l=0}^{\mathcal{L}-1} |h_l|^2) \tag{26}$$

and

$$D_f \ll s_f^2 (N_0 + N_x \sum_{l=0}^{\mathcal{L}-1} |h_l|^2) \tag{27}$$

$$\frac{\partial \mathrm{SINR}_j(\xi)}{\partial \xi} = 2NN_x(gs_o n - gs_o N - ns_f\xi)|\widetilde{h}_j|^2 \cdot \frac{gs_f s_o(s_f\xi - gs_o)(I(j,n) + N_0(Nn-n^2)) + (gs_o\xi D_f - s_f D_o)(Nn-n^2)}{((gs_o - s_f\xi)^2 I(j,n) + N(N_f^* n + N_o(N-n)))^2} \tag{24}$$

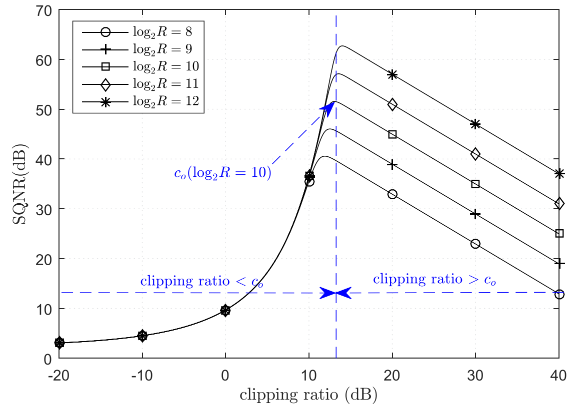

FIGURE 2. SQNR as a function of the clipping ratio for different resolutions of the ADC. The SQNR is much larger than 1 over a wide range of clipping ratios. SQNR decreases slowly when the clipping ratio is larger than c_o and rapidly when the clipping ratio is smaller than c_o.

From (22), the following back-of-the-envelope approximation is available

$$I(j,n) \approx N_x \sum_{l=0}^{\mathcal{L}-1} |h_l|^2 (Nn - n^2) \tag{28}$$

Substituting (28) into (26) and (27), we have

$$D_o(Nn - n^2) \ll g^2 s_o^2 (N_0(Nn - n^2) + I(j,n)) \tag{29}$$

and

$$D_f(Nn - n^2) \ll s_f^2 (N_0(Nn - n^2) + I(j,n)) \tag{30}$$

(29) and (30) can be used to simplify (25)

$$\begin{aligned} \xi_o &\approx \frac{s_f}{g s_o} \frac{g^2 s_o^2 (N_0(Nn - n^2) + I(j,n))}{s_f^2 (N_0(Nn - n^2) + I(j,n))} \\ &= g \frac{s_o}{s_f} \end{aligned} \tag{31}$$

The computational burden of (31) is reduced significantly compared to (25). $\xi_* = g s_o / s_f$ does not depend on the subcarrier index and is the preferred compensation factor to mitigate the ICI due to the gain adjustment in OFDM systems. When $\mathbb{Q}(y_0), \mathbb{Q}(y_1), \ldots, \mathbb{Q}(y_{n-1})$ are multiplied by ξ_*, the scalings of the received signal before and after the position of the gain adjustment are approximately the same. And the ICI is expected to be reduced significantly.

A. THE BEHAVIOR OF $\mathrm{SINR}_j(\xi_*)$ AS A FUNCTION OF n

In this subsection, we investigate the behavior of $\mathrm{SINR}_j(\xi_*)$ as a function of n. $\mathrm{SINR}_j(\xi_*)$ is given by

$$\mathrm{SINR}_j(\xi_*) = \frac{g^2 s_o^2 N N_x |\widetilde{h}_j|^2}{g^2 s_o^2 N N_0 + D_o(N-n) + g^2 s_o^2 D_f n / s_f^2} \tag{32}$$

Note that $(g s_o - s_f \xi_*)^2 I(j,n)$ is equal to zero. Thus the ICI is completely removed when ξ_* is chosen.

Take the partial derivation of $\mathrm{SINR}_j(\xi_*)$ to n, we have

$$\frac{\partial \mathrm{SINR}_j(\xi_*)}{\partial n} = \frac{g^2 s_o^2 s_f^2 N N_x |\widetilde{h}_j|^2 (D_o s_f^2 - g^2 s_o^2 D_f)}{(g^2 s_o^2 s_f^2 N N_0 + D_o s_f^2 (N-n) + g^2 s_o^2 D_f n)^2} \overset{\text{(I)}}{<} 0$$

where in step (I) we use (8). We can conclude that $\mathrm{SINR}_j(\xi_*)$ decreases with n. The settling time of the AGC should be as short as possible to increase $\mathrm{SINR}_j(\xi_*)$. This is consistent with the intuition.

IV. IMPLEMENTATION ISSUES

In this section, we discuss implementation issues of the proposed scheme. The clipping ratios before and after the position of the gain adjustment are estimated as $c_e = \sqrt{2/P'}$ and c_o respectively. The estimates of s_f and s_o are obtained as

$$s_f' = \sqrt{\frac{1}{\pi P'} \sum_{k=0}^{R-1} q_{k+1} (e^{-\frac{c_e^2 b_k^2}{2}} - e^{-\frac{c_e^2 b_{k+1}^2}{2}})} \tag{33}$$

and

$$s_o' = \sqrt{\frac{1}{\pi g^2 P'} \sum_{k=0}^{R-1} q_{k+1} (e^{-\frac{c_o^2 b_k^2}{2}} - e^{-\frac{c_o^2 b_{k+1}^2}{2}})} \tag{34}$$

And the estimate of ξ_* is obtained as

$$\xi_*' = \frac{\sum_{k=0}^{R-1} q_{k+1} (e^{-\frac{c_o^2 b_k^2}{2}} - e^{-\frac{c_o^2 b_{k+1}^2}{2}})}{\sum_{k=0}^{R-1} q_{k+1} (e^{-\frac{c_e^2 b_k^2}{2}} - e^{-\frac{c_e^2 b_{k+1}^2}{2}})} \tag{35}$$

From (35), we can conclude that ξ_*' is only a function of $\log_2 R$ and P'. Thus ξ_*' can be obtained by using the look-up table to reduce the computational complexity significantly. In general, P is not equal to P'. The ICI can not be completely removed with the proposed scheme in actual systems. The residual ICI is $(g s_o - s_f \xi_*')^2 I(j,n)$.

The resolution of the ADC $\log_2 R$ is usually fix at the receiver. We assume that the estimate of the received power P' is in the range $P^{\downarrow}$dB to $P^{\uparrow}$dB. If the resolution of the estimated power is P_R, then there is a total of $(P^{\uparrow} - P^{\downarrow})/P_R$ values in the look-up table. The memory of the look-up table is small. The proposed scheme only requires n complex multiplications. The computational complexity of the proposed scheme is low.

V. SIMULATION RESULTS

Simulations are carried out in this section to give numerical results of the proposed scheme and the traditional scheme. The transmission bandwidth is 1.4MHz, the sampling rate is 1.92MHz and the subcarrier spacing is 15kHz. The duration of the CP is equal to the delay spread of the channel. The channel models are the AWGN and the extended pedestrian A 5Hz (EPA5) with low spatial correlation [34]. The delay spreads of the AWGN channel and EPA5 channel are 0ns and 410ns respectively. For the state of the art, the settling time

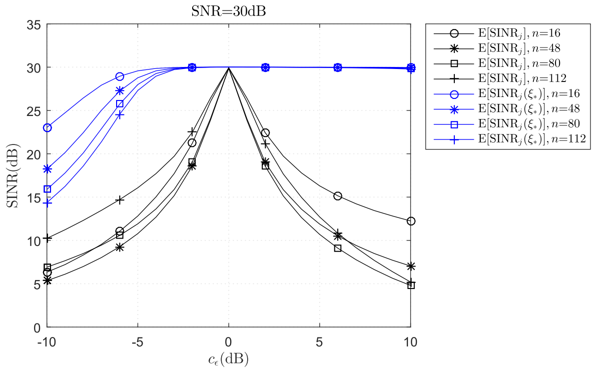

FIGURE 3. Comparison of E[SINR$_j$] and E[SINR$_j(\xi_*)$] as a function of c_ϵ for different n in the AWGN channel. We see that E[SINR$_j(\xi_*)$] is much larger than E[SINR$_j$].

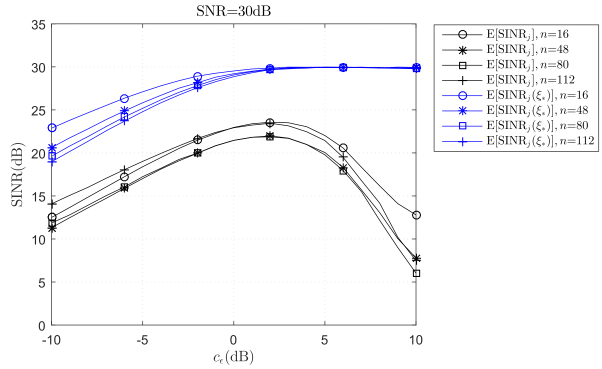

FIGURE 5. Comparison of E[SINR$_j$] and E[SINR$_j(\xi_*)$] as a function of c_ϵ for different n in the EPA5 channel. We see that E[SINR$_j(\xi_*)$] is much larger than E[SINR$_j$].

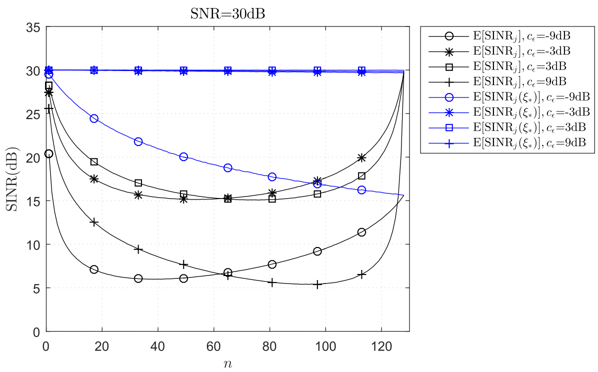

FIGURE 4. Comparison of E[SINR$_j$] and E[SINR$_j(\xi_*)$] as a function of n for different c_ϵ in the AWGN channel. We see that E[SINR$_j(\xi_*)$] is much larger than E[SINR$_j$].

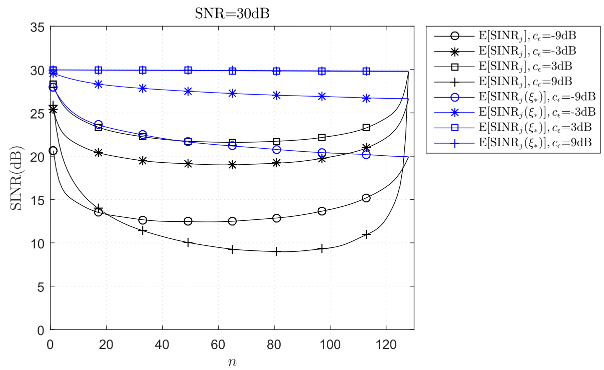

FIGURE 6. Comparison of E[SINR$_j$] and E[SINR$_j(\xi_*)$] as a function of n for different c_ϵ in the EPA5 channel. We see that E[SINR$_j(\xi_*)$] is much larger than E[SINR$_j$].

of the AGC is usually longer than these delay spreads. It is highly likely that the gain adjustment is carried out within the useful portion of the OFDM symbol. When evaluating the SINR performance, the signal-to-noise ratio (SNR) used in the simulations is 30dB, where SNR $= N_x \sum_{l=0}^{\mathcal{L}-1} \sigma_l / N_0$. The other parameters used in the simulations are: $N = 128$ and $\log_2 R = 10$.

A. SINR PERFORMANCE

In this subsection, the SINR performance is evaluated. The receiver is assumed to have a perfect estimate and a real estimate of the received power P respectively.

1) THE CASE $P' = P$

In the first part of this subsection, the receiver is assumed to have a perfect estimate of the received power P. The difference between the average clipping ratio before the position of the gain adjustment and the optimal clipping ratio is defined as

$$c_\epsilon \triangleq \sqrt{\frac{2}{N_x \sum\limits_{l=0}^{\mathcal{L}-1} \sigma_l + N_0}} - c_o \tag{36}$$

Fig. 3 compares E[SINR$_j$] and E[SINR$_j(\xi_*)$] as a function of c_ϵ for different n in the AWGN channel. In the traditional scheme, the cause of the ICI is due to the abrupt change of the DFT input. It is clear that this discontinuity increases with $|c_\epsilon|$. Thus, we see that E[SINR$_j$] first increases and then decreases with c_ϵ. And when $c_\epsilon = 0$, E[SINR$_j$] is maximized. The decrease in E[SINR$_j(\xi_*)$] is mainly due to an increase in the quantization error before the gain adjustment. The scenario of $c_\epsilon < 0$ is usually more seriously affected by the nonlinear effect of the ADC compared to the scenario of $c_\epsilon \geq 0$, as illustrated in Fig. 2. Thus, we see that E[SINR$_j(\xi_*)$] first increases with c_ϵ and then is close to the maximum value. If the proposed scheme is adopted in OFDM systems, the scenario of $c_\epsilon \geq 0$ is clearly preferred over the scenario of $c_\epsilon < 0$. In order to make the first scenario appears with high probability, the initial gain of the AGC should be low.

Fig. 4 compares E[SINR$_j$] and E[SINR$_j(\xi_*)$] as a function of n for different c_ϵ in the AWGN channel. E[SINR$_j$] first decreases and then increases with n. Let n_{MIN} be the position of the gain adjustment where E[SINR$_j$] is minimized. The receiver of the traditional scheme should avoid adjusting the power of the received signal at n_{MIN} and its vicinity. Both denominator and numerator of E[SINR$_j$] are a function of n.

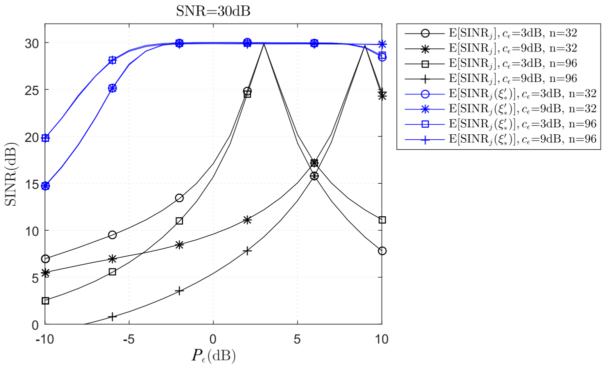

FIGURE 7. **Comparison of E[SINR$_j$] and E[SINR$_j(\xi'_*)$] as a function of P_ϵ for different n and c_ϵ in the AWGN channel. We see that E[SINR$_j(\xi'_*)$] is much larger than E[SINR$_j$].**

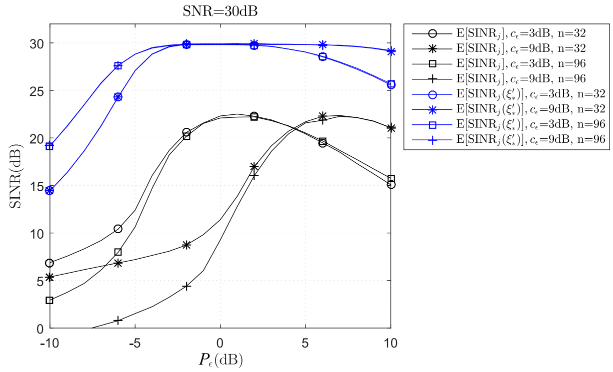

FIGURE 8. **Comparison of E[SINR$_j$] and E[SINR$_j(\xi'_*)$] as a function of P_ϵ for different n and c_ϵ in the EPA5 channel. We see that E[SINR$_j(\xi'_*)$] is much larger than E[SINR$_j$].**

Thus the position where E[SINR$_j$] is minimized usually does not coincide with the position where E[$I(j,n)$] is maximized. E[SINR$_j(\xi_*)$] decreases with n. This is consistent with the analysis in Section III.

Fig. 5 compares E[SINR$_j$] and E[SINR$_j(\xi_*)$] as a function of c_ϵ for different n in the EPA5 channel. Fig. 6 compares E[SINR$_j$] and E[SINR$_j(\xi_*)$] as a function of n for different c_ϵ in the EPA5 channel. We see that the behaviors of E[SINR$_j$] and E[SINR$_j(\xi_*)$] in the EPA5 channel are similar to those in the AWGN channel. In all the considered scenarios, E[SINR$_j(\xi_*)$] is much larger than E[SINR$_j$]. The proposed scheme increases the SINR significantly compared to the traditional scheme.

2) THE CASE $P' \neq P$

In the second part of this subsection, the receiver is assumed to have a real estimate of the received power P. The difference between the real estimate of the received power and the perfect estimate of the received power is defined as

$$P_\epsilon \triangleq P' - P \tag{37}$$

As mentioned above, the scenario of $c_\epsilon \geq 0$ is preferred over the scenario of $c_\epsilon < 0$. Thus the scenario of $c_\epsilon \geq 0$ is focused in the following simulations.

Fig. 7 compares E[SINR$_j$] and E[SINR$_j(\xi'_*)$] as a function of P_ϵ for different n and c_ϵ in the AWGN channel. In the traditional scheme, the difference between the scalings of the received signal before and after the position of the gain adjustment increases with $|P_\epsilon - c_\epsilon|$. Thus, we see that E[SINR$_j$] first increases and then decreases with P_ϵ. And when $P_\epsilon = c_\epsilon$, E[SINR$_j$] is maximized. A small estimation error of the received power results in a negligible reduction in E[SINR$_j(\xi'_*)$]. E[SINR$_j(\xi'_*)$] begins to decrease significantly when the estimation error exceeds a threshold. The power of the received signal usually can be estimated with a high degree of accuracy. Thus the proposed scheme has good performance in actual systems.

Fig. 8 compares E[SINR$_j$] and E[SINR$_j(\xi'_*)$] as a function of P_ϵ for different n and c_ϵ in the EPA5 channel. We see that the behaviors of E[SINR$_j$] and E[SINR$_j(\xi'_*)$] in the EPA5 channel are similar to those in the AWGN channel. In all the considered scenarios, E[SINR$_j(\xi'_*)$] is much larger than E[SINR$_j$]. The proposed scheme is more robust to P_ϵ compared to the traditional scheme.

B. BLER PERFORMANCE

To verify and validate the simulation results of the SINR performance, the block error ratio (BLER) performances of the traditional scheme and the proposed scheme are evaluated in this subsection. Channel coding is based on the third generation partnership project (3GPP) long term evolution (LTE) Turbo coding [35]. The code rate is 0.90 and the modulation scheme is 64 quadrature amplitude modulation (64QAM) using Gray mapping. The modulation symbols are mapped to W consecutive OFDM symbols, whose received powers can be assumed to be the same. In general, the received powers of these W consecutive OFDM symbols and the preceding OFDM symbol are different. When receiving these W consecutive OFDM symbols, the gain only needs to be adjusted in the first OFDM symbol.

The BLER performances of the traditional scheme and the proposed scheme in the AWGN channel are plotted in Fig. 9 and Fig. 10. The BLER performance of the traditional scheme decreases with $|P_\epsilon - c_\epsilon|$ and that of the proposed scheme is almost constant with respect to P_ϵ and c_ϵ. For the traditional scheme, the SINR is expected to decrease in the first OFDM symbol and is essentially unaffected by the nonlinear effect of the ADC in the second to the Wth OFDM symbol. For the proposed scheme, the SINR is essentially unaffected by the nonlinear effect of the ADC in all the W consecutive OFDM symbols. Thus, we see that the BLER performance of the traditional scheme increases with W and that of the proposed scheme is almost constant with respect to W. Ultra-reliable and low-latency communication (URLLC) is a type of service provided in 5G [36]. This type of service has a stringent requirement for latency. Low latency can be achieved by allowing data to be transmitted over few OFDM symbols, which results a small W.

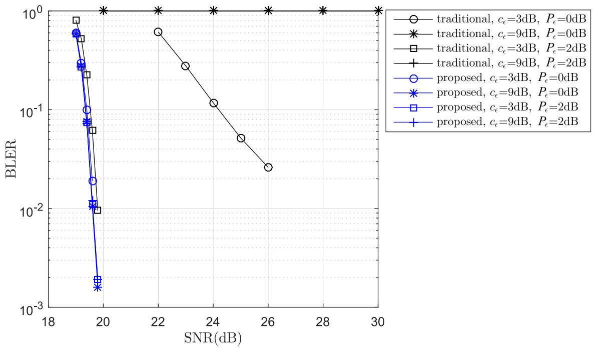

FIGURE 9. BLER performances of the traditional scheme and the proposed scheme in the AWGN channel. The number of transmit and receive antennas are 1 and 1 respectively. The other parameters are: $W = 6$ and $n = 32$.

The proposed scheme has a large advantage over the traditional scheme in this scenario.

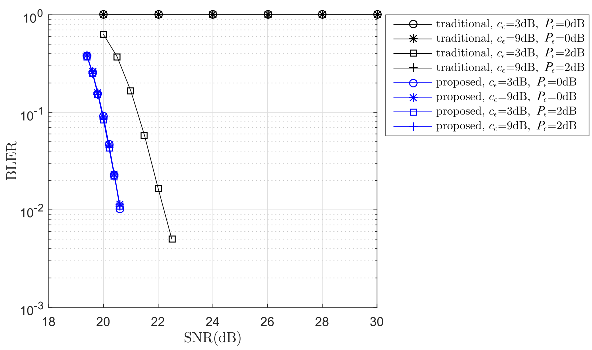

FIGURE 10. BLER performances of the traditional scheme and the proposed scheme in the AWGN channel. The number of transmit and receive antennas are 1 and 1 respectively. The other parameters are: $W = 1$ and $n = 32$.

The BLER performances of the traditional scheme and the proposed scheme in the EPA5 channel are plotted in Fig. 11 and Fig. 12. The behaviors of the BLER performances of the traditional scheme and the proposed scheme in the EPA5 channel are similar to those in the AWGN channel. In all the considered scenarios, the BLER performance of the proposed scheme is much better than that of the traditional scheme. This is consistent with the SINR performance.

VI. CONCLUSION

In this paper, we propose a simple and efficient scheme to mitigate the ICI due to the gain adjustment in OFDM systems. $\mathbb{Q}(y_0), \mathbb{Q}(y_1), \ldots, \mathbb{Q}(y_{n-1})$ are multiplied by a compensation factor before being fed into the DFT block. The compensation factor reduces the discontinuity of the received signal after the gain adjustment. The proposed scheme can be easily implemented in actual systems because of its low computational complexity. The simulation results show that the proposed scheme increases the SINR significantly compared to the traditional scheme.

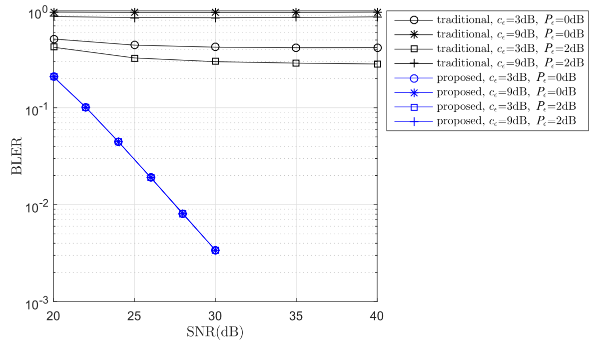

FIGURE 11. BLER performances of the traditional scheme and the proposed scheme in the EPA5 channel. The number of transmit and receive antennas are 1 and 2 respectively. The other parameters are: $W = 6$ and $n = 32$.

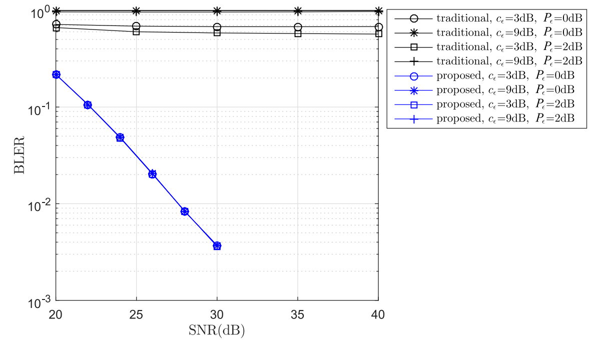

FIGURE 12. BLER performances of the traditional scheme and the proposed scheme in the EPA5 channel. The number of transmit and receive antennas are 1 and 2 respectively. The other parameters are: $W = 1$ and $n = 32$.

REFERENCES

[1] J. P. A. Pérez, S. C. Pueyo, and B. C. López, *Automatic Gain Control: Techniques and Architectures for RF Receivers*. New York, NY, USA: Springer, 2011.

[2] S. Ray and M. M. Hella, "A 10 Gb/s inductorless AGC amplifier with 40 dB linear variable gain control in 0.13μm CMOS," *IEEE J. Solid-State Circuits*, vol. 51, no. 2, pp. 440–456, Feb. 2016.

[3] C. Liu, Y. P. Yan, W. L. Goh, Y. Z. Xiong, L. J. Zhang, and M. Madihian, "A 5-Gb/s automatic gain control amplifier with temperature compensation," *IEEE J. Solid-State Circuits*, vol. 47, no. 6, pp. 1323–1333, Jun. 2012.

[4] J. P. A. Pérez, B. Calvo, and S. Celma, "A high-performance CMOS feedforward AGC circuit for a WLAN receiver," *IEEE Trans. Ind. Electron.*, vol. 57, no. 8, pp. 2851–2857, Aug. 2010.

[5] G. Jin, Y. Zhuang, M. Cui, Y. Yin, C. Li, and X. Xiang, "A stable and two-step settling digital controlled AGC loop for GNSS receiver," *IEICE Electron. Express*, vol. 11, no. 19, Sep. 2014, Art. no. 20140738.

[6] H. Zhang, G. Wang, and M. Lu, "Analysis and implementation of digital automatic gain control for DAB baseband decoder," *IEEE Trans. Consum. Eletron.*, vol. 57, no. 2, pp. 327–334, May 2011.

[7] H. Elwan, A. M. Soliman, and M. Ismail, "A CMOS Norton amplifier-based digitally controlled VGA for low-power wireless applications," *IEEE Trans. Circuits Syst. II, Analog Digit. Signal Process.*, vol. 48, no. 3, pp. 245–254, Mar. 2001.

[8] J. Wang, X. Hu, E. Guan, T. Li, Z. Ding, and Y. Yao, "A novel feed-forward segmented digital automatic gain control algorithm for long-term evolution digital radio-over-fibre systems," *IET Commun.*, vol. 11, no. 15, pp. 2362–2369, Oct. 2017.

[9] X. Cheng, G. Xie, Z. Zhang, and Y. Yang, "Fast-settling feedforward automatic gain control based on a new gain control approach," *IEEE Trans. Circuits Syst., II, Exp. Briefs*, vol. 61, no. 9, pp. 651–655, Sep. 2014.

[10] D. Tse and P. Viswanath, *Fundamentals of Wireless Communication*. New York, NY, USA: Cambridge Univ. Press, 2005.

[11] H. Wu, J. Li, B. Dai, and Y. Liu, "Analysis of the impact of AGC on cyclic prefix length for OFDM systems," *IEEE Trans. Commun.*, vol. 66, no. 10, pp. 4783–4794, Oct. 2018.

[12] H. Chae, I. Cho, and D. K. Kim, "Methods for mitigating inter-carrier interference caused by power amplifier transient in LTE modem," *IEICE Electron. Express*, vol. 12, no. 4, Feb. 2015, Art. no. 20141177.

[13] J. Lee, Q. Zhao, and H.-L. Lou, "Tracking automatic gain control of orthogonal frequency domain multiplexing systems," U.S. Patent 8 831 148 B1, Sep. 9, 2014.

[14] X. Liu, H.-H. Chen, X. Wang, and W. Meng, "Time domain precoding for OFDM/OFDMA systems without cyclic prefix," *IEEE Trans. Veh. Technol.*, vol. 67, no. 6, pp. 5510–5514, Jun. 2018.

[15] G. Berardinelli, "Generalized DFT-s-OFDM waveforms without cyclic prefix," *IEEE Access*, vol. 6, pp. 4677–4689, 2017.

[16] L. Samara, A. O. Alabassi, R. Hamila, and N. Al-Dhahir "Sparse equalizers for OFDM signals with insufficient cyclic prefix," *IEEE Access*, vol. 6, pp. 11076–11085, 2018.

[17] J.-B. Lim, C.-H. Choi, and G.-H. Im, "MIMO-OFDM with insufficient cyclic prefix," *IEEE Commun. Lett.*, vol. 10, no. 5, pp. 356–358, May 2006.

[18] J. H. Jang and H. J. Choi, "A fast automatic gain control scheme for 3GPP LTE TDD system," in *Proc. IEEE 72nd Veh. Technol. Conf. (VTC)*, Ottawa, CA, Canada, Sep. 2010, pp. 1–5.

[19] J. Li, V. Parizhsky, F. A. Lane, A. Jovicic, and Y. Wang, "Automatic gain control (AGC) for OFDM-based transmission in a wireless communication network," U.S. Patent 8 107 565 B2, Jan. 31, 2012.

[20] O.-E. Barbu, C. N. Manchón, C. Rom, T. Balercia, and B. H. Fleury, "OFDM receiver for fast time-varying channels using block-sparse Bayesian learning," *IEEE Trans. Veh. Technol.*, vol. 65, no. 12, pp. 10053–10057, Dec. 2016.

[21] T. L. Liu, W. H. Chung, S. Y. Yuan, and S. Y. Kuo, "ICI Self-Cancellation with cosine windowing in OFDM transmitters over fast time-varying channels," *IEEE Trans. Wireless Commun.*, vol. 14, no. 7, pp. 3559–3570, Jul. 2015.

[22] L. Rugini, P. Banelli, and G. Leus, "Simple equalization of time-varying channels for OFDM," *IEEE Commun. Lett.*, vol. 9, no. 7, pp. 619–621, Jul. 2005.

[23] P. Schniter, "Low-complexity equalization of OFDM in doubly selective channels," *IEEE Trans. Signal Process.*, vol. 52, no. 4, pp. 1002–1011, Apr. 2004.

[24] A. Aminjavaheri, A. Farhang, A. Rezazadehreyhani, L. E. Doyle, and B. Farhang-Boroujeny, "OFDM without CP in massive MIMO," *IEEE Trans. Wireless Commun.*, vol. 16, no. 11, pp. 7619–7633, Nov. 2017.

[25] Y. Mostofi and D. C. Cox, "Mathematical analysis of the impact of timing synchronization errors on the performance of an OFDM system," *IEEE Trans. Commun.*, vol. 54, no. 2, pp. 226–230, Feb. 2006.

[26] T. Araujo and R. Dinis, "Performance evaluation of quantization effects on multicarrier modulated signals," *IEEE Trans. Veh. Technol.*, vol. 56, no. 5, pp. 2922–2930, Sep. 2007.

[27] X. Zhang, Y. Zhao, and L. Zou, "Joint estimation of power and DC offset for OFDM systems based on distribution function," *Wireless Pers. Commun.*, vol. 56, no. 4, pp. 733–744, Feb. 2011.

[28] K.-P. Ho, "Maximum-likelihood power estimation for clipped signals," *IEEE Signal Process. Lett.*, vol. 16, no. 7, pp. 569–571, Jul. 2009.

[29] D. Dardari, "Joint clip and quantization effects characterization in OFDM receivers," *IEEE Trans. Circuits Syst. I, Reg. Papers*, vol. 53, no. 8, pp. 1741–1748, Aug. 2006.

[30] D. Dardari, V. Tralli, and A. Vaccari, "A theoretical characterization of nonlinear distortion effects in OFDM systems," *IEEE Trans. Commun.*, vol. 48, no. 10, pp. 1755–1764, Oct. 2000.

[31] A. Jeffrey and H. Dai, *Handbook of Mathematical Formulas and Integrals*, 4th ed. Burlington, MA, USA: Academic, 2008.

[32] J. Liu and H. Minn. (2015). *The Death of 5G Part 2: Will Analog be the Death of Massive MIMO?*. [Online]. Available: https://www.comsoc.org/ctn/death-5g-part-2-will-analog-be-death-massive-mimo

[33] Z. Song, X. Liu, X. Zhao, Q. Liu, Z. Jin, and B. Chi, "A low-power NB-IoT transceiver with digital-polar transmitter in 180-nm CMOS," *IEEE Trans. Circuits Syst. I, Reg. Papers*, vol. 64, no. 9, pp. 2569–2581, Sep. 2017.

[34] *Evolved Universal Terrestrial Radio Access (E-UTRA); Base Station (BS) Radio Transmission and Reception (Release 12)*, document 3GPP TS 36.104, V12.12.0, Dec. 2016.

[35] *Evolved Universal Terrestrial Radio Access (E-UTRA); Multiplexing and Channel Coding (Release 12)*, document 3GPP TS 36.212, V12.8.0, Mar. 2016.

[36] E. Dahlman, S. Parkvall, and J. Skold, *5G NR: The Next Generation Wireless Access Technology*. London, U.K.: Elsevier, 2018.

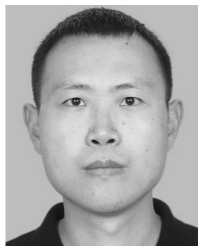

HAO WU received the M.S. degree in communication and information systems from Tianjin University, in 2009. He is currently a Senior Engineer with ZTE Corporation, Shenzhen, China. He has authored or co-authored several papers in international conferences and journals. He is the inventor of a number of patents. His research interests include wireless communications systems, digital signal processing, and error control coding.

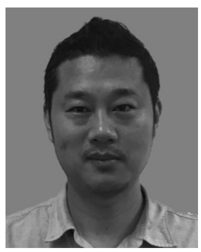

JUN LI received the M.S. degree from the Nanjing University of Science and Technology, Nanjing, China, in 2006. He is currently a Senior Engineer with ZTE Corporation, Shenzhen, China. His research interests include digital signal processing, array processing, and baseband algorithms.